JOURNAL OF CATALYSIS 148, 625–638 (1994)

Preparation, Structural Properties, and Hydrogenation Activity of Highly Porous Palladium–Titania Aerogels

M. Schneider, M. Wildberger, M. Maciejewski, D. G. Duff, T. Mallát, and A. Baiker[1]

Department of Chemical Engineering and Industrial Chemistry, Swiss Federal Institute of Technology, ETH-Zentrum, 8092 Zürich, Switzerland

Received December 17, 1993; revised March 4, 1994

Mesoporous to macroporous palladium–titania aerogels with high surface area have been synthesized by the sol–gel–aerogel route. A titania gel was prepared by the addition of an acidic hydrolysant to tetrabutoxytitanium(IV) in methanol. The palladium precursor solutions, added after the redispersion of the titania gel, were either Na_2PdCl_4, $(NH_4)_2PdCl_4$, $Pd(acac)_2$, or $Pd(OAc)_2$ dissolved in protic or aprotic solvents. The palladium–titania aerogels have a BET surface area of 170–190 $m^2 g^{-1}$ after a thermal treatment up to 673 K and contain well-developed anatase crystallites of about 7–8 nm mean size. Depending on the palladium precursor used, the volume-weighted-mean particle size, determined by TEM, varies significantly in the range 21–224 nm, this being independently consistent with XRD line-broadening results. All aerogel samples showed pronounced structural stability of both the titania matrix and the palladium particles towards the pretreatment media used (air or hydrogen) at temperatures up to 773 K. Thermal analysis, combined with mass spectrometry, revealed that the untreated catalysts contain a considerable amount of entrapped organic impurities after high-temperature supercritical drying. Liquid-phase hydrogenations of *trans*-stilbene and benzophenone were used as test reactions for characterizing the activity and accessibility of the palladium particles. A comparison of the best dispersed $Pd(OAc)_2$-derived aerogel catalysts with conventionally impregnated titania-supported palladium catalysts in the liquid-phase hydrogenation of 4-methylbenzaldehyde reveals superior activity and selectivity for the aerogel catalysts. © 1994 Academic Press, Inc.

INTRODUCTION

The potential of aerogels for catalysis resides in their unique morphological and chemical properties (1–3). These originate from their wet chemical preparation by the solution–sol–gel (SSG) method (4) and the subsequent removal of solvent via supercritical drying (SCD). Due to the "structure-preserving" ability of SCD (5), the aerogels are usually solids of high porosity and specific surface area. Mixed gels of *in situ* reduced Group VIII metals, highly dispersed and uniformly distributed in different metal oxide matrices are readily synthesized by this combination of the SSG-technology with ensuing SCD (6–8).

Based on our previously published method for synthesis of meso- to macroporous titania aerogels with high surface area (9), we recently demonstrated the direct preparation of highly dispersed Pt–titania aerogels possessing marked structural stability and excellent hydrogenation activity (6). This and the increasing academic as well as commercial interest in titania-supported Group VIII metal catalysts (especially for carbonyl-group hydrogenation) (10–12) prompted us to extend our studies to palladium–titania aerogel catalysts.

Applying the same method for the wet chemical SSG-process as in Ref. (6), consisting of preformation of the titania gels and their subsequent redispersion followed by the addition of different Pd precursor solutions before SCD, we aimed to prepare stable, mesoporous palladium–titania aerogels with high specific surface areas. For testing the accessibility and activity of the palladium particles, the liquid-phase hydrogenations of *trans*-stilbene (Eq. [1]), benzophenone (Eq. [2]), and 4-methylbenzaldehyde (Eq. [3]) were chosen:

$$\text{Ph–CH=CH–Ph} \xrightarrow{+H_2} \text{Ph–CH}_2\text{–CH}_2\text{–Ph} \qquad [1]$$

$$\text{Ph–CO–Ph} \xrightarrow{+H_2} \text{Ph–CHOH–Ph} \qquad [2]$$

$$\xrightarrow[-H_2O]{+H_2} \text{Ph–CH}_2\text{–Ph}$$

$$\text{4-CH}_3\text{–C}_6\text{H}_4\text{–CHO} \xrightarrow{+H_2} \text{4-CH}_3\text{–C}_6\text{H}_4\text{–CH}_2\text{OH} \qquad [3]$$

$$\xrightarrow[-H_2O]{+H_2} \text{4-CH}_3\text{–C}_6\text{H}_4\text{–CH}_3.$$

trans-Stilbene, benzophenone, and 4-methylbenzaldehyde are all bulky molecules favoured by catalysts with wide pores and they possess different functional groups

[1] To whom correspondence should be addressed.

0021-9517/94 $6.00

(C=C double bond or carbonyl group). In addition to the low-temperature liquid-phase hydrogenation, which is especially suitable for bulky molecules, we also investigated the effects of different pretreatment procedures on the structural and catalytic properties.

EXPERIMENTAL

Sol–Gel–Aerogel Synthesis

Throughout the text the following scheme of abbreviations is used, taking Pd5PAc as an example. The numeral following "Pd" designates the Pd content in wt% and the subsequent letters represent the Pd precursor used ($(Na_2PdCl_4 \rightarrow$ PC; $(NH_4)_2PdCl_4 \rightarrow$ NP; $Pd(acac)_2 \rightarrow$ PA; $Pd(OAc)_2 \rightarrow$ PAc). These acronyms describe the original (untreated) aerogel materials.

Analytical grade reagents were used throughout this work. The preparation of the palladium–titania aerogels is derived from that for Pt–titania reported in Ref. (6), and consequently only a short description will be given here. The SSG process was carried out in an anti-adhesive, closed Teflon beaker, under nitrogen atmosphere and at ambient temperature (297 ± 2 K). First, the acidic hydrolysant diluted with methanol was added to a methanolic solution of tetrabutoxytitanium(IV). The resulting titania gels were aged for 4 h and then redispersed with different amounts of methanol (Table 1). The Pd precursor solution (Table 1) was added to the nonviscous titania solution and a second ageing step for 19 h under vigorous stirring followed (ca. 1000 rpm). With Pd2PC and Pd2NP, red–orange translucent solutions developed, while in the case of Pd2PA the solution was yellow and translucent. With Pd2PAc and Pd5PAc, the initially red–orange colour turned to dark green and then black within minutes. These solutions were highly viscous in the case of Pd2PC and Pd2NP.

The as-prepared sol–gel product was transferred in a Pyrex-glass liner into an autoclave with a net volume of 1.09 l together with the appropriate amount of additional methanol (outside of the liner) (Table 1), thus exceeding the critical volume of the mixed solvent (solvent volume ca. 375 ml in all cases). The corresponding critical data for methanol, as the dominating component of all five SSG-solvents, are V_c = 118 ml mol^{-1}, T_c = 513 K, and p_c = 8.1 MPa (13). The SCD conditions were set as follows (6): nitrogen prepressure of 5 MPa, heating rate of 1 K min^{-1} to final SCD temperature of 533 K, 30 min thermal equilibration (final pressure about 19 MPa) and isothermal depressurization with 0.1 MPa min^{-1}. As represented in Table 1, the precursor solution of Pt2PA contained 30 ml of benzene (T_c = 562 K (14)), which was compensated for by a 5 K increase of the SCD end-temperature. The resulting grey aerogel clumps were then ground in a mortar.

Finally, portions of the untreated (raw) aerogel powders were thermally treated in a tubular reactor with upward flow. The media applied were air, air followed by hydrogen or hydrogen. The pretreatment temperatures ranged from 473 to 773 K. Detailed descriptions of the single pretreatment processes are given in Ref. (6). The only exceptions are the thermal treatments of two Pd2PA samples calcined in the same way as the standard air treatment, but at temperatures of 723 and 773 K, respectively. Moreover, portions of Pd2PA, Pd2PAc, and Pd5PAc were heated in air at 1 K min^{-1} and kept at 373 K for 8 h. Then the temperature was increased to 473 K at 0.5 K min^{-1} and held for 11 h.

The metal loading was generally calculated on the basis of the nominal amounts used (Table 1) and the assumption of a complete reduction of the Pd precursors. The nominal metal loadings were independently confirmed by oxidation–decomposition analysis. The assumption of the complete reduction is justified on the basis of published data (15) concerning the preparation of Pd sols in refluxing methanol (338 K and ambient pressure). Note that we used 533 K and a methanolic pressure of ca. 10 MPa.

Nitrogen Physisorption

The specific surface areas (S_{BET}), mean cylindrical pore diameters ($\langle d_p \rangle$) and specific adsorption pore volumes

TABLE 1

Compositions of the Palladium Precursor Solutions, Amount of Methanol (MeOH) Used for the Redispersion of the Titania Gels and Extra Amount of MeOH Added for the Supercritical Drying

Aerogel	Precursor (mg)	Solvent composition (ml)	MeOH for redispersion (ml)	Extra MeOH for SCD (ml)
Pd2PC	$PdCl_2$ (256) NaCl (168)	H_2O (1.0)/ MeOH (24)	71	130
Pd2NP	$(NH_4)_2PdCl_4$ (410)	H_2O (2)/MeOH (24)	71	130
Pd2PA	$Pd(acac)_2$ (440)	Benzene (30)	71	124
Pd2PAc	$Pd(OAc)_2$ (324)	Acetone (24) (warm)	71	130
Pd5PAc	$Pd(OAc)_2$ (835)	Acetone (40) (warm)	55	130

(V_{pN_2}) were derived from nitrogen physisorption measurements at 77 K using a Micromeritics ASAP 2000 instrument. Prior to measurement, all samples were degassed to 0.1 Pa at 423 K. BET surface areas were calculated in a relative pressure range of 0.05 to 0.2 assuming a cross-sectional area of 0.162 nm^2 for the nitrogen molecule. The pore size distributions were calculated applying the Barrett–Joyner–Halenda (BJH) method (16) to the desorption branches of the isotherms (17). The assessments of microporosity were made from *t*-plot constructions ($0.3 < t < 0.5$ nm), using the Harkins–Jura correlation (18).

X-Ray Diffraction

X-ray powder diffraction (XRD) patterns were measured on a Siemens Θ/Θ D5000 powder X-ray diffractometer. The diffractograms were recorded with detector-sided Ni-filtered $K\alpha$Cu radiation over a 2Θ-range of 20° to 90° and a position-sensitive detector. The mean crystallite sizes were determined using the Scherrer equation (19) and the (101)- or (200)-reflection for anatase (20), the (111)-reflection for Pd (21), and the (110)-reflection for PdO (22).

Transmission Electron Microscopy

Samples for transmission electron microscopy (TEM) were loaded dry onto perforated, thin carbon films supported on copper grids, aerogel powder being poured five times onto the carbon film and shaken off.

Diffraction-contrast TEM was performed using a Hitachi H-600 electron microscope operated at 100 kV, with a point resolution of ca. 0.5 nm. The instrumental magnification had previously been calibrated using the phase contrast from catalase crystals. Identification of the palladium component used its usually greater contrast in comparison to the less electron-dense titania, as well as the different particle morphologies. However, where the palladium size data overlapped with the size range of the anatase primary crystallites (5–11 nm), identification was hardly possible due to the rather limited and orientation-dependent contrast differences. The evaluation and representation of the measured particle size distribution is described in more detail in Ref. (6).

Briefly, the most important parameters obtained from the distribution data were the mean diameter from the volume-weighted ($\langle d \rangle_v$) and the mean diameter from the (surface-)area-weighted distribution ($\langle d \rangle_a$). The number of palladium particles measured varied from 25 to 44. The breadth of the size distributions was expressed by the coefficient of variation, the root-mean-square (standard) deviation of diameters from the (unweighted) mean expressed as a (percent) fraction of this mean.

Thermal Analysis

TG and DTA investigations were performed on a Netzsch STA 409 instrument coupled with a Balzers QMG 420/QMA 125 quadrupole mass spectrometer, equipped with Pt–Rh thermocouples and Pt crucibles. A heating rate of 10 K min^{-1} and an air flow of 25 ml min^{-1} were used. The sample weight was ca. 32 mg and the α-Al_2O_3 reference weight 62.5 mg.

Total carbon and hydrogen contents were determined with a LECO CHN-900 elemental microanalysis apparatus.

Catalytic Characterization

Trans-stilbene and benzophenone hydrogenation were performed at 303 and 343 K, respectively, and at atmospheric hydrogen pressure. Isopropylacetate (*trans*-stilbene) and butylacetate (benzophenone) were used as solvents. The semibatch apparatus and experimental procedure, as well as the analysis of the product mixtures were described in detail in a previous report (6).

To minimize the influence of side reactions, the initial rates were determined from reactant consumption at below 5% conversion. Preliminary tests with the most active aerogel catalyst, in which the amount of catalyst, stirring speed and granule fraction were varied within a wide range showed that the reaction rate in [mol s^{-1} $(g_{Pd})^{-1}$] was independent of the amount of catalyst (≤50 mg), the stirring speed (≥500 rpm) as well as the particle size (≤500 μm), indicating that interparticle and intraparticle mass transfer control could be ruled out. For a few of the most active catalysts the experimental errors of the catalytic testing were determined, estimated from three consecutive measurements. They ranged between 5 and 10%.

The hydrogenation of 4-methylbenzaldehyde was performed in the same semi batch apparatus as mentioned above. A 1 wt% ethanolic solution of 4-methylbenzaldehyde was hydrogenated with 10–30 mg aerogel powder (<300 μm) at 35 ml min^{-1} hydrogen flow (atomspheric pressure) and 333 ± 1 K. The Pd : reactant weight ratio was kept constant at 1 : 40. Samples of the reaction mixture (ca. 0.3 ml) were periodically taken, filtered, and analyzed using gas chromatography (6).

RESULTS

Properties of the palladium-titania aerogels are listed in Table 2.

Nitrogen Physisorption

Figure 1 depicts as a representative example the adsorption/desorption isotherms and differential pore size distribution of the Pd5PAc sample, calcined in air at 573 K. All aerogel samples showed a type-IV isotherm with a type-H1 desorption hysteresis according to IUPAC-classification (23). They all possess pronounced meso- to macroporosity and only little microporosity, yielding pore-

TABLE 2

Properties of the "Palladium"–Titania Aerogel Catalysts Pretreated in Air and/or Hydrogen at Different Temperatures

Aerogel/pretreatment temperature			S_{BET} (S_t)	$\langle d_p \rangle$	V_{pN_2}	XRD-crystallinity and		$\langle d \rangle_v$
	in air (K)	in hydrogen (K)	(m^2/g)[a]	(nm)[b]	(cm^3/g)	$\langle d_c \rangle$ (nm)[c]		(nm)[d]
Pd2PC/	—	—	—	—	—	A/Pd	7.2/28	224
	573	—	190 (13)	21	1.00	A/Pd/PdO	7.3/30/—	—
	673	—	180 (13)	22	0.99	A/Pd/PdO	7.3/29/—	168
Pd2NP/	—	—	—	—	—	A/Pd	7.5/28	—
	573	—	183 (11)	22	0.98	A/Pd	7.6/30	—
	673	—	174 (10)	21	0.92	A/Pd/PdO	7.8/28/—	—
Pd2PA/	—	—	—	—	—	A/Pd-C	7.4/12	130
	473	—	187 (9)	19	0.88	A/Pd	7.6/13	—
	573	—	180 (10)	20	0.90	A/Pd/PdO	7.6/15/—	104
	673	—	173 (9)	21	0.89	A/PdO/Pd	7.7/—/—	114
	723	—	167 (9)	22	0.89	A/PdO	7.9/—/—	111
	773	—	148 (9)	23	0.86	A/PdO	8.3/—	—
Pd2PAc/	—	—	—	—	—	A/Pd–C	7.2/9.6	46
	473	—	192 (8)	19	0.89	A/Pd/PdO	7.5/9.5/—	—
	573	—	181 (10)	22	1.01	A/PdO/Pd	7.4/—/—	—
	673	—	173 (10)	20	0.87	A/PdO	7.5/—	49
Pd5PAc/	—	—	—	—	—	A/Pd–C	7.3/9.1	21
	473	—	191 (11)	20	0.93	A/Pd/PdO	7.8/9.6/—	—
	573	—	183 (11)	22	0.96	A/PdO/Pd	7.5/—/—	—
	673	—	176 (11)	19	0.85	A/PdO	7.6/—	22
	573	573 k	176 (11)	22	0.98	A/Pd	7.7/10.5	—
	573	673 k	164 (9)	22	0.91	A/Pd	8.1/10.9	—
	—	473 k	187 (4)	20	0.95	A/Pd	7.7/9.3	—
	—	673 k	172 (10)	23	0.98	A/Pd	7.9/10.0	—

[a] (S_t) in parenthesises specific micropore surface area derived from *t*-plot analysis.

[b] $\langle d_p \rangle = 4V_{pN_2}/S_{BET}$.

[c] A (anatase); Pd, PdO, Pd–C (solid solution of carbon in Pd) in order of decreasing intensity; $\langle d_c \rangle$ corresponding mean crystallite sizes (—, not determinable with calculation reliability <20 %).

[d] $\langle d \rangle_v$ volume-weighted-mean TEM particle sizes for the 'palladium' component consisting of Pd, Pd–C, and/or PdO.

size maxima of about 50 nm and specific micropore surface areas (estimated from the corresponding *t*-plot analysis) of up to 13 $m^2 g^{-1}$. The pore size distributions derived from the desorption branch (17) were all very broad and asymmetric (Fig. 1). This property is also apparent if one compares the graphically assessed pore size maxima (ca. 50 nm) with the mean cylindrical pore sizes $\langle d_p \rangle$ given in Table 2.

Pretreatments in air and/or hydrogen up to 673 K led to S_{BET} of 169 to 192 $m^2 g^{-1}$ and V_{pN_2} of 0.85 to 1.01 $cm^3 g^{-1}$ with almost constant microporosity. This thermal stability of all aerogel catalysts is additionally represented by the Pd2PA series calcined in air up to 773 K. Increasing the calcination temperature from 473 to 773 K caused a reduction of S_{BET} by only 20%, whereby V_{pN_2} remains virtually constant around 0.9 $cm^3 g^{-1}$.

X-Ray Diffraction

The X-ray patterns of the raw aerogels are represented in Fig. 2. The crystalline fraction of the titania is generally made up of well-developed anatase crystallites (20). The mean anatase crystallite sizes range from 7.2 to 8.3 nm, being virtually independent of the pretreatment medium used and the temperature up to 773 K. Depending on the precursor solution employed, either metallic palladium, Pd, (Pd2PC, Pd2NP) or an interstitial solid solution of carbon in palladium, Pd–C, (Pd2PA, Pd2PAc, Pd5PAc) is formed. The formation of this solid solution has been observed by several authors (24–26). In the present case, the interstitial Pd–C solution causes a uniform expansion of the cubic Pd lattice. In all raw aerogels derived from organometallic precursors, the Pd lattice constant in-

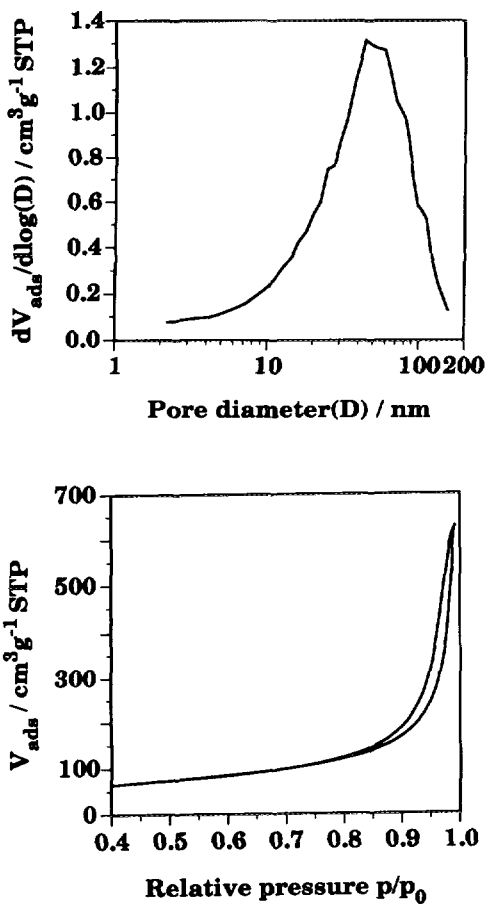

FIG. 1. Textural properties of the Pd5PAc catalyst calcined at 573 K. Bottom: adsorption/desorption isotherms (STP; 273.15 K, 1 atm); top: differential pore size distribution.

creased from 3.8898 to 3.9959 Å corresponding to an approximate atomic ratio of carbon to Pd of about 0.15 (24, 26). The expansion results in a shift of the Pd (111) reflection to lower 2Θ values by 1.115° and corresponding shifts in the other Pd reflections. The X-ray diffraction patterns shown in Fig. 2 and the mean crystallite sizes ($\langle d_c \rangle$) listed in Table 2 indicate that, depending on the Pd precursor solution used, different $\langle d_c \rangle$ values for the palladium component were obtained. In contrast to our previous results for Pt–titania aerogel catalysts (6), the chloridic Pd precursors led to larger mean crystallite sizes ($\langle d_c \rangle \approx 30$ nm) than the organometallic precursors ($\langle d_c \rangle \approx 10$ nm Pd2PAc, Pd5PAc; $\langle d_c \rangle \approx 13$ nm Pd2PA).

Oxidative treatments in the temperature range of 473 to 773 K led generally to an increasing fraction of PdO. The PdO formation proceeded either directly from Pd or from Pd–C via Pd (decomposition of solid solution) (Fig. 2). For the aerogels (Pd2PA, Pd2PAc, Pd5PAc), which contained the Pd–C solid solution, calcination in air at 473 K for 11 h was sufficient to remove carbon from the Pd lattice (Table 2) (24, 26). The oxidizability of the Pd as a function of the volume-weighted-mean particle size is apparent in Fig. 3, which depicts the X-ray diffraction patterns of Pd2PC, Pd2PA, and Pd5PAc samples after calcination in air at 673 K. Note that the smaller the mean particle size, the higher the proportion of PdO formed. The Pd5PAc sample with a mean particle size of about 20 nm shows only PdO, whereas Pd2PA with about 100 nm mean particle size reaches complete oxidation only at 773 K. Figure 4 shows a selection of Pd5PAc samples treated in air and/or hydrogen at temperatures up to 673 K. Apart from the calcination in air at 473 and 673

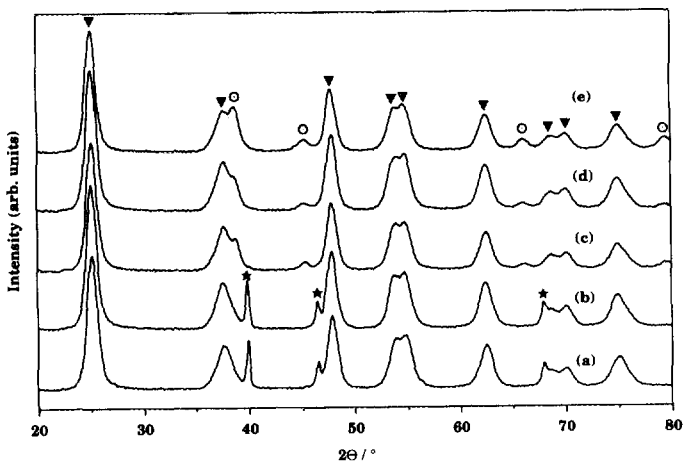

FIG. 2. X-ray diffraction patterns (Cu $K\alpha$) of the raw aerogels: (a) Pd2PC, (b) Pd2NP, (c) Pd2PA, (d) Pd2PAc, and (e) Pd5PAc. (▼) anatase, (★) Pd, and (⊙) Pd–C. Designations of the samples are explained in the Experimental section.

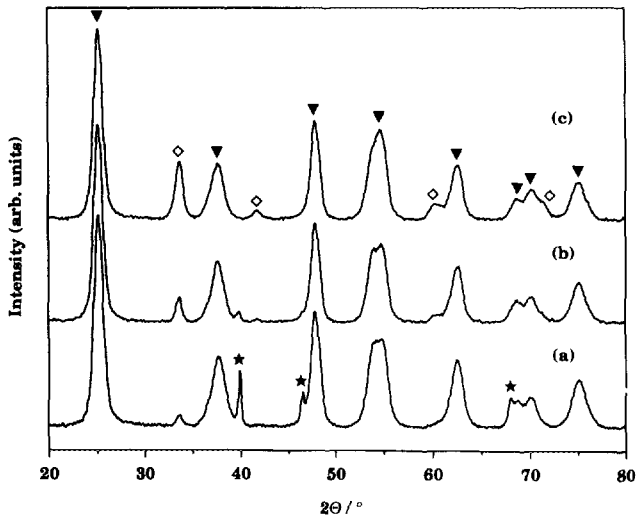

FIG. 3. X-ray diffraction patterns (Cu $K\alpha$) of aerogel catalysts, all calcined in air at 673 K: (a) Pd2PC, (b) Pd2PA, and (c) Pd5PAc. (▼) anatase, (★) Pd, and (◇) PdO.

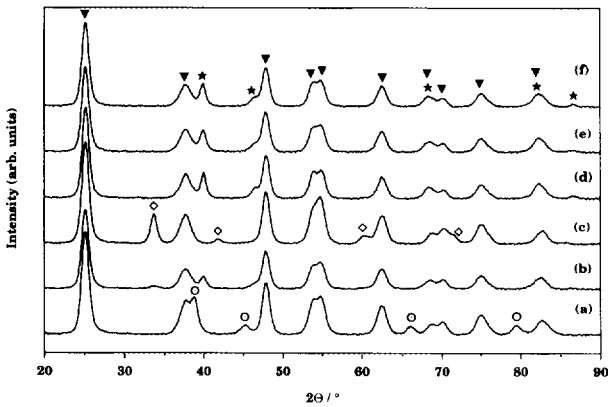

FIG. 4. X-ray diffraction patterns (Cu $K\alpha$) of the Pd5PAc series calcined in air and/or hydrogen at various temperatures: (a) raw, (b) air 473 K, (c) air 673 K, (d) air 573 K followed by hydrogen 673 K, (e) hydrogen 473 K, and (f) hydrogen 673 K. (▼) anatase, (★) Pd, (◎) Pd–C, and (◇) PdO.

K, which results in the transformation of Pd–C to Pd followed by its complete oxidation to PdO, it is also evident that hydrogen treatments at temperatures above 473 K (the lowest reduction temperature investigated) led to metallic Pd.

Transmission Electron Microscopy

It has already emerged from the XRD studies that the catalysts can contain "palladium" in the form of Pd, Pd–C, and/or PdO. With respect to the identification of these "palladium" particles it can be stated that the diffraction-contrast identification is valid in all cases and that the corresponding particle size enlargements of Pd–C and PdO are negligible, lying in the precision range of the particle size determination. With Pd–C, the approximate particle size increase amounts to about 3% and with PdO to about 17%. Transmission electron micrographs of raw Pd2PC and a portion of Pd2PC calcined in air at 673 K, which contains a considerable amount of PdO besides Pd, are represented in Fig. 5. A closer inspection of the edges of "palladium" particles reveals that the calcination at 673 K resulted in the formation of rougher contours showing more diffuse edges, presumably due to the partially oxidized Pd component. Diffraction-contrast TEM im-

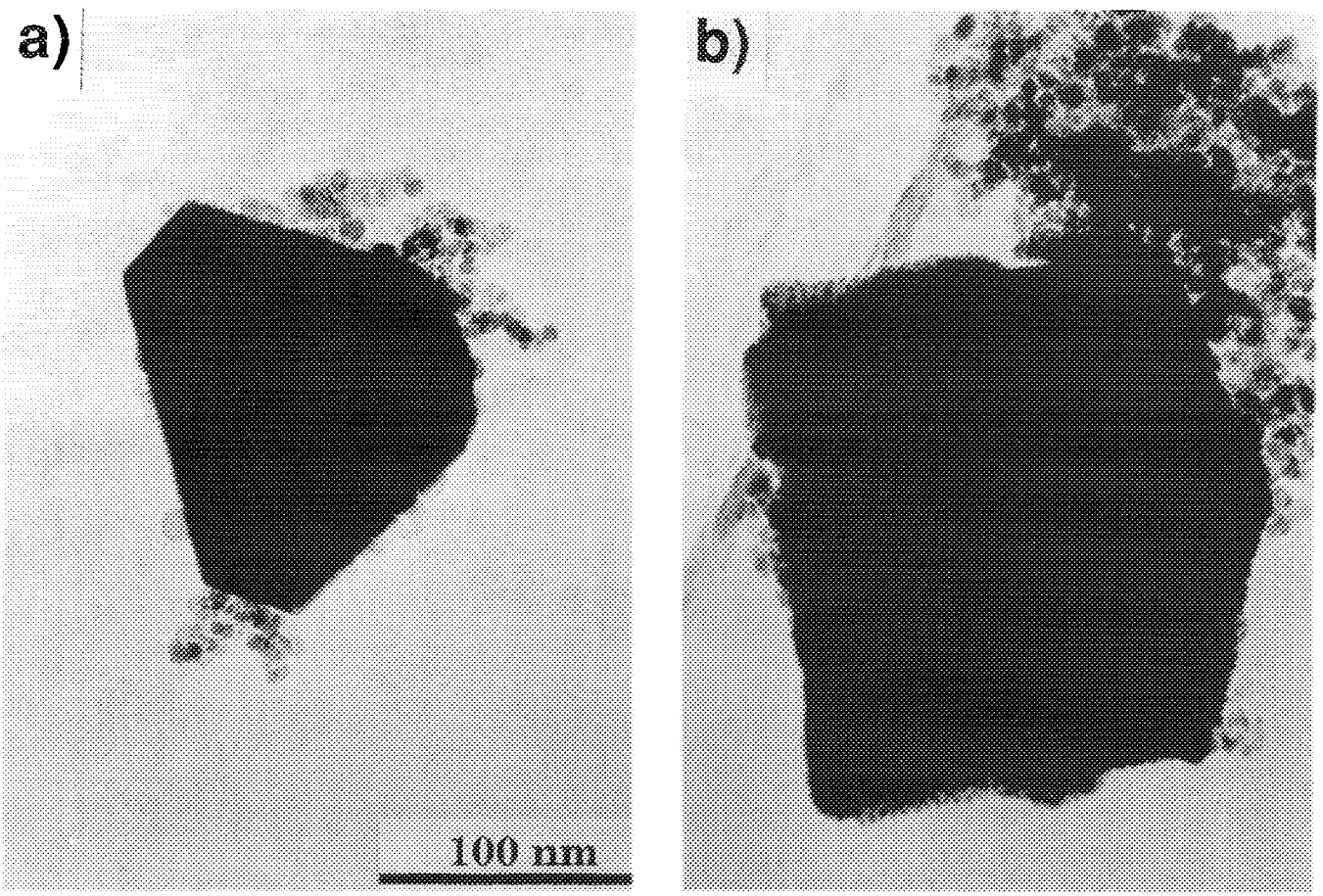

FIG. 5. Diffraction-contrast TEM images of Pd2PC samples: (a) raw and (b) calcined in air at 673 K.

ages from the raw aerogels Pd2PC, Pd2PA, Pd2PAc, and Pd5PAc are shown in Fig. 6. In all cases the large smooth dark contrast features, frequently showing anisotropic shapes, are assumed to be the "palladium" particles usually standing out against the much finer titania matrix which has a primary-particle size distribution of 5–11 nm (6). However, with the more dispersed samples, especially those derived from $Pd(OAc)_2$, it was difficult to identify unequivocally many of the "palladium" particles, due to the insufficient contrast difference in the titania matrix size range. Moreover, TEM revealed no "palladium" species in all samples studied, which were smaller than the primary titania particles (in contrast to the situation for Pt (6)). Such small particles are most probably sintered during the thermal pretreatment process.

The often irregular shapes and internal contrasts seen in the diffraction-contrast TEM images (Fig. 5) indicate a great degree of polycrystallinity. This is confirmed by comparing the mean crystallite sizes and the volume-weighted-mean particle sizes determined by XRD and TEM, respectively (Table 2). In Pd2PC there are also a number of more regular particle outlines present, compatible with more crystalline species bound predominantly by (111) surface planes. Decahedral multiply-twinned, octahedral (e.g., Fig. 6a) and singly-twinned (Fig. 5) structural properties are among those suggested by these particle projections (27). The absence of strongly irregular particle profiles (long and thin) of either "palladium" or titania in the micrographs shows that the particle shapes must also be relatively isotropic (near-spherical, cubic, and/or decahedral, for example) in three dimensions, there being no preferred orientation with respect to the electron beam in these samples.

The particle size distributions from the diffraction-contrast TEM micrographs of the raw aerogel samples are shown in Fig. 7. In agreement with XRD line-broadening experiments, the TEM data show that medium dispersions were achieved with the precursors $Pd(OAc)_2$ at 2 and especially 5 wt%. In contrast, poor dispersions were obtained with $Pd(acac)_2$ and especially Na_2PdCl_4. The coefficients of variation for all size data determined were between 27 and 56%.

Particle size distributions for portions of Pd2PA both raw and following different pretreatments in air are presented in Fig. 8. Considering the rather high uncertainty of these particle size distributions, we see no significant change or evidence of sintering of the large "palladium" particles, which is also corroborated by the $\langle d \rangle_v$ values and the results from X-ray diffraction (Table 2). The differing $\langle d \rangle_v$ values for Pd2PC presented in Table 2 are not in agreement with the corresponding XRD-derived mean crystallite sizes, which are fairly constant. This discrepancy is due to a single larger particle from a larger mode being present on the micrograph of the raw sample, but statistically absent in the images of the material calcined at 673 K.

In brief, the TEM images demonstrate a distinct heterogeneity with wide and possibly multimodal particle size distributions. Thus the error on the mean particle size values may amount to 30–50%.

Thermal Analysis

The thermal analysis was performed in flowing air for a series of both raw and differently pretreated Pd5PAc samples. Figure 9 depicts the results of thermal analysis for the raw aerogel Pd5PAc. All Pd5PAc samples, whether raw or pretreated in air and/or hydrogen, show essentially comparable thermoanalytical properties. The weight losses originate from the oxidation of organic residues, mainly stemming from the alkoxylation of the oxidic surface during SCD, and from the evolution of water (desorption of physisorbed water, dehydroxylation). This conclusion emerges from relating the TG curve with the monitored ion intensities of CO_2^+ (m/z = 44) and H_2O^+ (m/z = 18) (Fig. 9). Based on a comparison of the size of recorded water and CO_2 releases from the differently pretreated Pd5PA samples, it is evident that the dominance of the evolved-water contribution to the overall weight losses increases with increasing pretreatment temperature. The evolution of water began at room temperature and reached maxima at about 393 and 518 K, as illustrated in Fig. 9. The H_2O evolution at the beginning originates mainly from physisorbed water and is later dominated by the contribution of water from oxidation of the organics. As mentioned previously, a distinct decrease of the content of organic residues, reflected by decreasing intensities of the CO_2 traces, was reached with any thermal treatment up to 673 K, which was in fact virtually independent of the pretreatment medium (air or hydrogen) used (Fig. 10). Independent of both the pretreatment medium and the temperatures used, two stages of CO_2 evolution were detected for the whole Pd5PAc series, as illustrated in Fig. 10, and also observed with Pt–titania aerogels (6). This indicates the presence of two "kinds" of organic species in the aerogel samples investigated. The first stage of CO_2 evolution started at ca. 390–450 K and attained a maximum at 541 K with a subsequent maximum at 613 K. With the raw sample there was an additional maximum at 458 K (Fig. 9). From about 790 K, a second stage of CO_2 production occurred reaching its maximum at 973 K. In accordance with this, the DTA curves are dominated by two broad exothermic signals related to the corresponding oxidation of organic residues and thus formation of CO_2 (Fig. 9). The low-temperature stage, dominating in the raw sample, stems predominantly from organic species mainly covering the accessible surface and thus being the first to be removed. A part of the organic residues, which

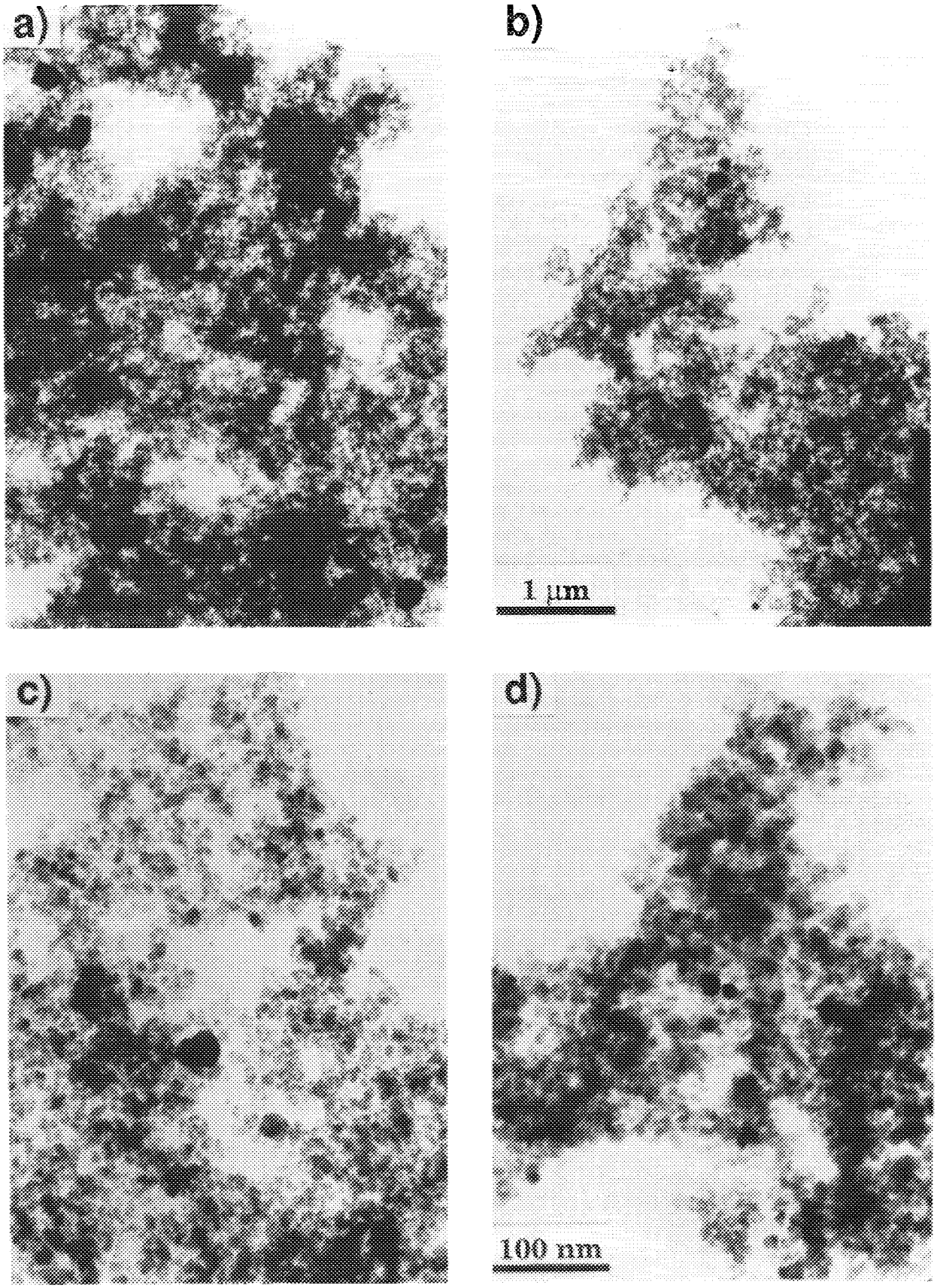

FIG. 6. Diffraction-contrast TEM images of the uncalcined aerogels: (a) Pd2PC (b), Pd2PA, (c) Pd2PAc, and (d) Pd5PAc. (a) is at the same scale as (b), and (c) is the same as (d).

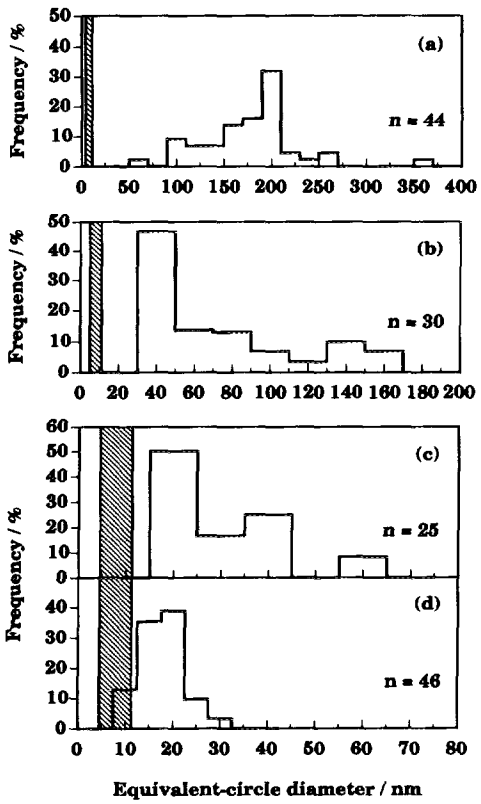

FIG. 7. Particle size distributions derived from TEM for the raw samples: (a) Pd2PC, (b) Pd2PA, (c) Pd2PAc, and (d) Pd5PAc. The hatched area marks the primary-particle size distribution of titania.

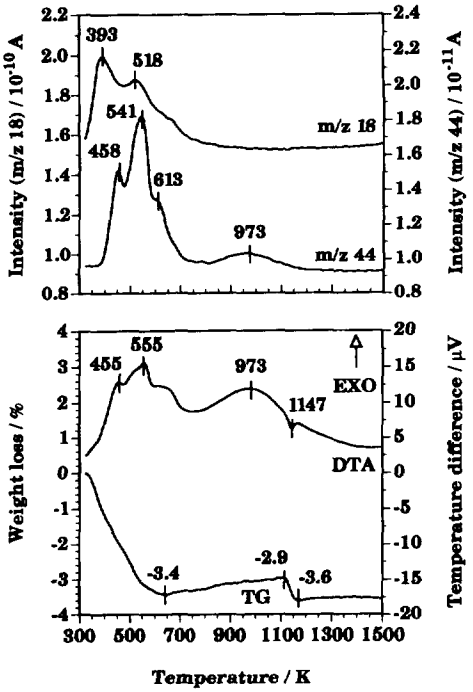

FIG. 9. Results of thermoanalytical investivation of the raw aerogel Pd5PAc. Bottom: TG and DTA curves; top: ion intensities of $m/z(CO_2^+)$ = 44 (CO_2) and $m/z(H_2O^+)$ = 18 (water). Heating rate, 10 K min^{-1}; air flow, 25 ml min^{-1}.

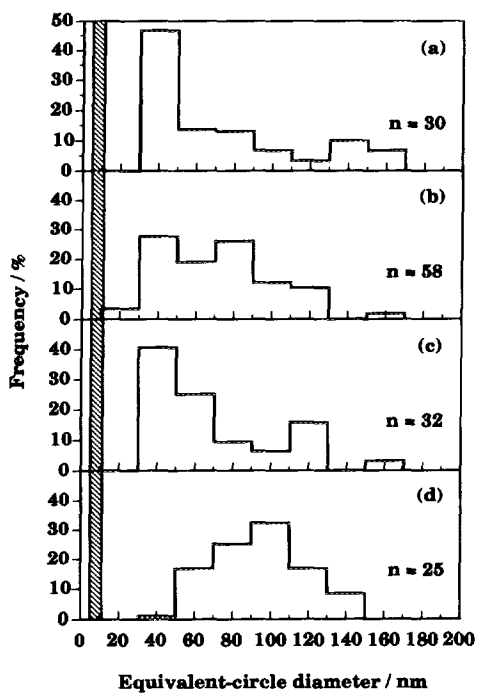

FIG. 8. Particle size distributions derived from TEM for the Pd2PA series calcined in air at different temperatures: (a) raw, (b) 573 K, (c) 673 K, and (d) 723 K. The hatched area marks the primary-particle size distribution of titania.

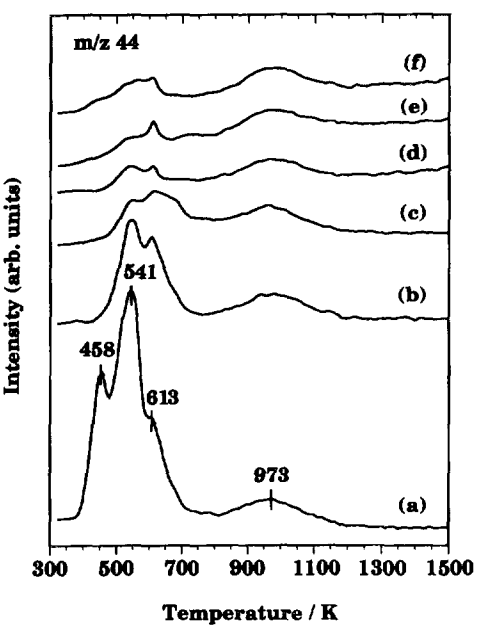

FIG. 10. CO_2-evolution ($m/z(CO_2^+)$ = 44) during thermoanalytical runs from Pd5PAc catalysts, treated in air and/or hydrogen at different temperatures: (a) raw, (b) air 473 K, (c) air 573 K, (d) air 673 K, (e) air 573 K followed by hydrogen 673 K, and (f) hydrogen 673 K. Heating rate, 10 K min^{-1}; air flow, 25 ml min^{-1}.

evolved during the first stage, revealed a high thermal resistance towards treatments in air and/or hydrogen up to 673 K. This behaviour can be attributed to organic residues sitting deep in the porous titania matrix. Their removal is most probably controlled by diffusion. The high-temperature stage of CO_2 evolution, arising at about 790 K, can be attributed to organics being predominantly incorporated in the titania matrix and thus hardly affected by the pretreatment procedures applied. Consequently, even after a treatment at 673 K for 5 h the samples still contain detectable amounts of both types of organic residues, estimated to be less than 5% of the amount in the raw sample.

At about 660 K, the oxidation of Pd, related to the weight uptake in the TG curve, began to dominate over the CO_2 and H_2O evolution (Fig. 9). Such a weight increase was only observed with the raw and the reduced samples, which contained predominantly Pd–C and Pd, respectively. With all Pd5PAc catalysts investigated, the resulting PdO subsequently started to decompose at ca. 1100 K with an endothermic DTA peak at 1147 K.

For raw Pd2PC and Pd2NP, the aerogels derived from chloridic Pd precursors (Table 1), the carbon contents from elemental microanalysis amounted to 1.6 and 1.9 wt%, respectively. In the cases of raw Pd2PA, Pd2PAc, and Pd5PAc, all three derived from organometallic precursors, the carbon contents were about 1.1 wt%. The hydrogen contents were similar for all the raw samples (ca. 0.9 wt%) and represent a superposition of water originating from the oxidation of the organic residues and water, already present in either physisorbed or chemisorbed form. The carbon contents thus indicate that all raw aerogels contain a considerable amount of organic residues after high-temperature SCD. This is mainly attributed to the realkoxylation of titanium-bound hydroxyl groups (4, 6, 28). Probably to a lower extent, some organic oxidation products (precursor reduction) as well as organic species decomposed over Pd must also be taken into account.

Hydrogenation Activity

The catalytic behaviour of "palladium"–titania aerogels in the liquid-phase hydrogenation of *trans*-stilbene and benzophenone is summarized in Table 3. The initial reaction rates have been calculated on a Pd weight basis (r_0 = [mol s^{-1} $(g_{Pd})^{-1}$]).

The effects of the catalytic runs on the catalyst composition were investigated. The pretreatment in hydrogen at the reaction temperatures of any (partly) oxidized catalyst caused an immediate colour change from yellow or yellow–red to dark grey, indicating the formation of metallic Pd. Corresponding XRD investigations after the catalytic tests of a portion of Pd2PAc and Pd5PAc, both treated in air at 673 K and consequently containing predominantly PdO, revealed that the reductive conditions applied resulted in the formation of metallic Pd. However, with raw Pd5PAc, the XRD analysis indicated that neither *trans*-stilbene hydrogenation at 303 K nor benzophenone hydrogenation at 343 K had influenced the Pd–C solid solution formed during SCD.

A comparison of the reaction rate data (Table 3) for the reactions tested indicates that all "palladium"–titania catalysts studied showed significantly higher initial rates for the hydrogenation of the C=C double bond in trans-stilbene at a lower hydrogenation temperature.

In contrast to our experience with similarly prepared Pt–titania catalysts (6), the aerogel catalysts derived from chloridic Pd precursors possess very poor dispersions ($\langle d \rangle_v > 150$ nm), independently determined by XRD and TEM, and hence negligible initial rates both in trans-stilbene and especially benzophenone hydrogenation (Table 3). The "palladium"–titania catalysts derived from organometallic precursors showed area-weighted-mean particle sizes ranging from ca. 19 to 116 nm and correspondingly decreasing hydrogenation activity. The best dispersed Pd2PAc and especially Pd5PAc samples possess remarkable activities even in their raw states. With raw Pd5PAc, the initial rates were about half of the maximum initial rates, which were obtained after oxidative pretreatment for both *trans*-stilbene and benzophenone hydrogenation.

The increase of the loading from 2 to 5 wt% in the $Pd(OAc)_2$-derived samples with the corresponding changes in the aerogel preparation of Pd5PAc led to beneficial changes in both the mean particle size and the initial reaction rate. Thus, unexpectedly, the "palladium" particle size distribution seems to be shifted to lower particle size by the increased precursor concentration. Pd5PAc had a significantly smaller mean particle size and the initial rates were the highest among the catalysts examined.

Generally, any oxidative pretreatment increased the initial activity in *trans*-stilbene and benzophenone hydrogenation. With the aerogel catalysts derived from organometallic precursors, the benefit of an oxidative pretreatment was already apparent at 473 K. The Pd5PAc catalyst, calcined in air at 473 K, showed the highest r_0 for *trans*-stilbene hydrogenation of all the catalysts investigated. Moreover, for the Pd2PA series the initial activities increased further with the pretreatment temperature up to 723 K. Thus the Pd2PA catalysts showed the most pronounced influence of an oxidative pretreatment on the catalytic performance, resulting in an increase of r_0 by a factor of about 50. The rise in activity is most likely to be due to the oxidative removal of a fraction of organic impurities from the PdO–Pd surface.

The pretreatments in hydrogen, however, did not seem to be beneficial, as revealed by the series of Pd5PAc samples differently treated in hydrogen. When calcination

TABLE 3

Liquid-Phase Hydrogenation of *trans*-Stilbene (303 K) and Benzophenone (343 K) at Atmospheric Pressure

Aerogel/pretreatment temperature			$\langle d \rangle_a$[a]	$r_0 \times 10^5$	
	in air (K)	in hydrogen (K)	(nm)	(mol/s/g_{Pd}) *trans*-Stilbene	Benzophenone
Pd2PC/	—	—	207	0.1	0
	573	—	—	0.8	—
	673	—	167	1.3	0
Pd2NP/	—	—	—	0.1	—
	573	—	—	0.2	—
	673	—	—	0.3	—
Pd2PA/	—	—	116	0.4	0
	473	—	—	2.0	0
	573	—	95	3.7	—
	673	—	101	7.5	—
	723	—	106	17.7	3.0
	773	—	—	15.3	—
Pd2PAc/	—	—	41	6.8	0.8
	473	—	—	21.0	3.2
	573	—	—	25.2	—
	673	—	45	25.3	4.5
Pd5PAc/	—	—	20	35.3	3.8
	473	—	—	74.7	7.2
	573	—	—	53.7	—
	673	—	19	59.3	8.2
	573	573	—	36.5	3.7
	573	673	—	35.3	2.5
	—	473	—	52.5	4.2
	—	673	—	15.5	1.3

Note. Initial rates (r_0) and area-weighted-mean particle sizes ($\langle d \rangle_a$) are shown.
[a] Derived from TEM. (see Experimental section)

in air did not precede the hydrogen treatment, the detrimental influence of the latter was even more pronounced.

Table 4 shows the catalytic data for 4-methylbenzaldehyde hydrogenation (reaction (3)) over Pd2PAc and Pd5PAc catalysts, both calcined in air at 673 K. Literature data for a low acidity and high acidity 0.5 wt% titania-supported Pd catalyst are included for comparison (29). These catalysts were prepared by impregnation of titania extrudates (phase ratio of anatase : rutile = 3 : 1), subsequent calcination in air and reduction under a H_2–N_2 atmosphere. The tests were carried out using the same Pd : reactant ratio as in Ref. (29). The results indicate that the aerogel catalysts possess much higher hydrogenation activity (Table 4). Almost full conversion to 4-methylbenzyl alcohol could be achieved in 0.5–1 h at considerably lower temperature and hydrogen pressure. The hydroxymethyl group of the benzyl alcohol derivative is subsequently converted to the corresponding methyl group. Note that the reduction of aromatic aldehydes on Pd is generally faster than the further reduction of the intermediate aromatic alcohols (30). Another interesting point is the negligible formation of ethyl 4-methylbenzyl ether after 4 h (Table 4). The catalytic tests indicate that the aerogel catalysts are very active in the reduction of the carbonyl group in 4-methylbenzaldehyde to the corresponding hydroxyl group and in the hydrogenolysis of the C–O bond to form hydrocarbons, but ethyl 4-methylbenzyl ether formation is negligible due to the absence of strong acidic sites.

DISCUSSION

Structural Aspects

The meso- to macroporosity of the "palladium"–titania aerogels make them particularly interesting for appli-

TABLE 4

Catalytic Activity of Palladium–Titania Catalysts in the Liquid-Phase Hydrogenation of 4-Methylbenzaldehyde (a) to 4-Methylbenzyl Alcohol (b), *p*-Xylene (c), and Ethyl 4-Methylbenzyl Ether (d)

Catalyst	Time (h)	Temp. (K)	Pressure (MPa)[a]	Product composition (%) (a)	(b)	(c)	(d)
Pd2PAc	1	333	0.05	3	80	17	0
(calcined in air at 673 K)	4	333	0.05	2	12	86	0
Pd5PAc	0.5	333	0.05	3	95	2	0
(calcined in air at 673 K)	4	333	0.05	3	18	79	0
0.5 wt% Pd/TiO_2 (Pd 6)[b]	4	423	1	5	15	71	7
0.5 wt% Pd/TiO_2 (Pd 1C)[b]	4	423	1	26	0	0	73

[a] Hydrogen partial pressure.
[b] From Ref. (29): sample Pd 6 is a weakly acidic and Pd 1C is a strongly acidic catalyst.

cation in liquid-phase reactions. Similar textural properties were also found for Pt-titania aerogels (6). Wide pores make the high internal surface area more accessible for the bulky reagents.

The morphological and textural stability of the titania matrix and the stability of the "palladium" crystallites (XRD) and particles (TEM) towards sintering are further beneficial properties of our "palladium"–titania systems.

Another interesting aspect, emerging from this study, is the presence of a solid solution of carbon in Pd determined for aerogels prepared with organometallic Pd precursors, i.e., $Pd(acac)_2$ and $Pd(OAc)_2$. A likely explanation is that the organic ligands of the organometallic precursors are the carbon source being liberated during the nucleation and/or particle growth. They are decomposed, deposited and incorporated into Pd during the course of SCD.

The various factors which can influence the resulting particle size distributions have been discussed in a previous paper (6), in which the same general metal component precursor classes (chloridic and organometallic metal complexes) have been used. The dispersions are generally lower for "palladium"–titania catalysts than for Pt–titania catalysts. A striking difference between these aerogels is that the influence of the metal precursor on the final metal particle sizes shows just the opposite behaviour. With "palladium"–titania the smallest mean particle sizes are achieved using organometallic precursors, and with Pt–titania using chloridic Pt precursors. This finding illustrates the difficulty of predicting the outcome of the metal particle distribution. In our work on Pt–titania aerogels (6) we tried to rationalize the genesis of the metallic particles in metal-metal oxide aerogels. There the observed colours indicated that the platinum ions remained unreduced upon mixing the Pt salts with the methanolic titania suspensions. Thus the metal reduction and the particle formation occurred mainly during the high-temperature SCD. With the $Pd(OAc)_2$-derived aerogels used in this work, the colour of the wet chemical stage turned to black within minutes after the addition of the Pd precursor solution. A possible reason for this behaviour could be that the formation of the metallic particles occurs predominantly via homogeneous nucleation. This suggestion is supported by the increase of dispersion with increasing loading in the preparation of Pd5PAc. It seems that the increased metal precursor concentration in the sol–gel process resulted in a higher nucleation rate, which is considered to be a determining factor in producing small, monodisperse particles. We can conclude that in the system presented here, the homogeneous nucleation seems to be an important mechanism dominating at least part of the aerogel preparations.

Catalytic Aspects

The prehydrogenation step (at reaction conditions) used in the catalytic tests reduces the PdO fraction in the calcined catalysts before the addition of the reactant. After the reaction, only metallic Pd was detected by XRD analysis, as already mentioned in the catalytic section. Thus the catalytic tests reflect the behaviour of the aerogels with palladium in the metallic state.

A comparison of the initial rates for *trans*-stilbene and benzophenone hydrogenation, studied both with "palladium"–titania and recently published Pt–titania aerogel catalysts (6), show a marked difference. The chloride-derived Pt–titania catalysts do not specifically favour either benzophenone or *trans*-stilbene hydrogenation,

whereas both the chloridic-derived and organometallic-derived "palladium"–titania catalysts prefer unequivocally *trans*-stilbene hydrogenation. Despite the significantly larger mean particle sizes of "palladium"–titania compared to Pt–titania aerogels (6), higher initial rates are measured for trans-stilbene hydrogenation over "palladium"–titania. Note that the best dispersed Pd–titania catalyst shows up to seven times higher initial activity. This favourable catalytic performance is unlikely to be due to beneficial metal–support interaction. It is well known that the nature of the substituents on a reactant molecule can considerably affect the reducibility of a functional group (30). Kazanskii and Tatevosyan (31) showed that in contrast to the effect on platinum and nickel aryl groups increased the ease of C=C double bond hydrogenation over palladium.

With the "palladium"-titania catalysts, the oxidative treatments at temperatures between 473 and 723 K caused a marked activity increase for all samples studied. In contrast, with the related Pt–titania catalysts a beneficial effect arose only with $PtCl_4$-derived aerogels oxidatively pretreated at 573 K or above. This behaviour seems to be related to the oxidizability of the "palladium" component mentioned in the XRD section. PdO occurs in the temperature range 473–673 K. When compared with the corresponding raw catalysts, pretreatment in air followed by hydrogen had either no significant influence (*trans*-stilbene hydrogenation) or detrimental effects (benzophenone hydrogenation). This behaviour was found for "palladium"–titania and Pt–titania aerogels (6). Prereductions of selected Pt–titania samples in pure hydrogen at 473 and 673 K, without preceding calcination in air, resulted in a continuous activity decrease for both reactions. With the Pd–titania aerogel catalysts, subjected to the same prereduction, such detrimental effects only occurred with prereductions at 673 K. A possible explanation for this behaviour is that with hydrogen pretreatments (especially at 673 K) the beneficial effect of the removal of the organic residues is superseded by the formation of TiO_x overlayers (11, 12), which partially cover the active Pd surface. Another explanation could be partial sintering and/or morphological changes of the Pd particles, which cannot be ruled out completely based on the TEM analysis. It is also possible that further contaminants (chlorine, nitrogen) present in Pd2PC and Pd2NP may play a role; however, they are unlikely to be the major factor influencing the hydrogenation activity, as the results of the different pretreatments (oxidative, reductive) (6, 32) indicate.

As shown by XRD studies of raw Pd5PAc after both *trans*-stilbene and benzophenone hydrogenation, the Pd–C solution persists during the catalytic testing and indicates that not only metallic Pd but also the Pd–C phase exhibit a remarkable, but somewhat lower hydrogenation activity.

CONCLUSIONS

The present studies demonstrate that high-surface-area "palladium"–titania aerogels with meso- to macroporosity can be synthesized by high-temperature SCD. Both the "palladium" particles and the titania matrix possess a remarkable structural stability up to 773 K. By varying the Pd precursor solution, different "palladium" particle size distributions can be obtained. The catalytic studies show that the activities, expressed as mol s^{-1} $(g_{Pd})^{-1}$, are much higher for the hydrogenation of *trans*-stilbene than those for the benzophenone hydrogenation. The best dispersed "palladium"–titania aerogels, derived from $Pd(OAc)_2$, show superior activity and selectivity for 4-methylbenzaldehyde hydrogenation compared to impregnated titania-supported Pd catalysts.

REFERENCES

1. Schneider, M., and Baiker, A., *in* "Encyclopedia of Advanced Materials" (D. Bloor, R. J. Brook, M. C. Flemings, and S. Mahajan, Eds.), Vol. 1. Pergamon, Oxford, 1994.
2. Ko, E. I., *CHEMTECH* **23**(4), 31 (1993).
3. Pajonk, G. M., *Appl. Catal.* **72,** 217 (1991).
4. Brinker, C. J., and Scherer, G. W., "Sol–Gel Science, the Physics and Chemistry of Sol–Gel Processing." Academic Press, San Diego, 1990.
5. Scherer, G. W., *J. Am. Ceram. Soc.* **73,** 3 (1990).
6. Schneider, M., Duff, D. G., Mallát, T., Wildberger, M., and Baiker, A., *J. Catal.* **147,** (1994).
7. Mizushima, Y., and Makoto, H., *Eur. Mater. Res. Soc. Monogr.* **5,** 195 (1993).
8. Armor, J. N., Carlson, E. J., and Zambri, P. M., *Appl. Catal.* **19,** 339 (1985).
9. Schneider, M., and Baiker, A., *J. Mater. Chem.* **2,** 587 (1992).
10. "Preprints, 3rd International Symposium Fine Chemistry Catalysis, Heterogeneous Catalysis and Fine Chemicals, Poitiers, 1993."
11. Tauster, S. J., *Acc. Chem. Res.* **20,** 389 (1987).
12. Tauster, S. J., Fung, S. C., Baker, R. T. K., and Horseley, J. A., *Science* **211,** 1121 (1981).
13. The Thermodynamics Research Center, The Texas A&M University System, "TRC Thermodynamic Tables—Non-Hydrocarbons," Vol. IV, p. i-5000. College Station, TX, 1992.
14. The Thermodynamics Research Center, The Texas A&M University System, "TRC Thermodynamic Tables—Hydrocarbons," Vol. III, p. i-3200. College Station, TX, 1992.
15. Hirai, H., Nakao, Y., and Toshima, N., *J. Macromol. Sci.-Chem.* **A13,** 727 (1979).
16. Barrett, E. P., Joyner, L. G., and Halenda, P. P., *J. Am. Chem. Soc.* **73,** 373 (1951).
17. Broekoff, J. C. P., *in* "Preparation of Heterogeneous Catalysts" (B. Delmon, P. Grange, P. Jacobs and G. Poncelet, Eds.), p. 663. Elsevier, Amsterdam, 1979.
18. Harkins, W. D., and Jura, G., *J. Chem. Phys.* **11,** 431 (1943).
19. Klug, H. P., and Alexander, L. E., "X-Ray Diffraction Procedures for Polycrystalline and Amorphous Materials." p. 656. Wiley, New York, 1974.
20. JCPDS Mineral Powder Diffraction Data File 21-1272. Park Lane, PA.
21. JCPDS Mineral Powder Diffraction Data File 5-0681. Park Lane, PA.

22. JCPDS Mineral Powder Diffraction Data File 6-0515. Park Lane, PA.
23. Sing, K. S. W., Everett, D. H., Haul, R. A. W., Moscou, L., Pierotti, R. A., Rouquérol, J., and Siemieniewska, T., *Pure Appl. Chem.* **57,** 603 (1985).
24. Maciejewski, M., and Baiker, A., *J. Phys. Chem.*, **98,** 285 (1994).
25. Stachurski, J., and Frackiewicz, A., *J. Less-Common Met.* **108,** 249 (1985).
26. Ziemecki, S. B., Jones, G. A., Swartzfager, D. G., Harlow, R. L., and Faber, J., *J. Am. Chem. Soc.* **107,** 4547 (1985).
27. Kirkland, A. I., Edwards, P. P., Jefferson, D. A., and Duff, D. G., *Ann. Rep. Prog. Chem.* **87,** 247 (1990).
28. Prassas, M., Phalippou, J., and Zarzycki, J., *J. Mater. Sci.* **19,** 1656 (1984).
29. Bankmann, M., Brand, R., Freund, A., and Tacke, T., *in* "Preprints, 3rd International Symposium Fine Chemistry Catalysis, Heterogeneous Catalysis and Fine Chemicals, Poitiers, 1993," p. C 75.
30. Freifelder, M., "Practical Catalytic Hydrogenation Techniques and Application." Wiley, New York, 1971.
31. Kazanskii, B. A., and Tatevosyan, G. T., *J. Gen. Chem. USSR* **9,** 2256 (1939).
32. Wieckowski, A., *in* "Modern Aspects of Electrochemistry" (R. E. White, J. O'M. Bockris and B. E. Conway, Eds.), Vol. 21, p. 3. Plenum, New York, 1990.